Composites: Part B 42 (2011) 155–166

Contents lists available at ScienceDirect

Composites: Part B

journal homepage: www.elsevier.com/locate/compositesb

Performance of sandwich composites subjected to sequential impact and air blast loading

Matthew Jackson [a], Arun Shukla [b,*]

[a] Naval Undersea Warfare Center, Newport, RI 02841, United States
[b] Dynamic Photo-Mechanics Laboratory, Department of Mechanical Industrial and Systems Engineering, The University of Rhode Island, Kingston, RI 02881, United States

ARTICLE INFO

Article history:
Received 21 June 2010
Received in revised form 23 August 2010
Accepted 14 September 2010
Available online 21 September 2010

Keywords:
A. Layered structures
B. Debonding
B. Impact behavior
Blast loading

ABSTRACT

An experimental study has been conducted to examine the effects of two different types of impact damage on the blast performance of sandwich composites. Sandwich composite specimens were subjected to impact by either a high velocity projectile or a low velocity drop weight. After impact, a secondary blast loading experiment was performed on the same specimens to evaluate the effects of the impact damage on the blast performance of the sandwich. Controlled blast loading was imparted using a shock tube apparatus while pressure data and high speed images of the dynamic event were captured. The experimental results showed impact damage from high velocity projectiles was most prominent on the exit face sheet of the sandwich specimens wherein damage to the core and impact face sheet, in the form of a hole, was minimal in comparison. Damage created by low velocity drop weights was concentrated on the impact face sheet and within the core adjacent to the impact face sheet. Low velocity impacts also generated de-bonding between the impact face sheet and core. Shear cracking in the core was the dominant effect of all blast loading.

Although the specimens that had been struck by high velocity projectiles absorbed substantially more energy during impact experiments than those impacted by low velocity drop weights the damage created by low velocity impacts had the greatest detrimental effect on the blast performance of the sandwich composites.

1. Introduction

Blast loading events are a constant threat for military structures including ships, vehicles, and buildings. Due to increasing terrorist threats, non-military structures have come under greater threat of blast loading events in recent years. These threats have lead to a greater interest in sandwich structures that perform better during blast events than traditional materials and offer the additional benefit of a high strength to weight ratio allowing for additional armor to be installed on military vehicles.

In normal service, structures constructed with sandwich composites will likely experience events that will degrade the shock mitigation properties of the sandwich composite structure. This includes long duration exposure to UV light, thermal cycling or short duration events, namely impact. Impact events are placed into two categories, namely, high velocity impacts with low mass or low velocity impact with high mass. High velocity impact damage may be generated by gun fire, or in conjunction with a blast event that produces shrapnel. Low velocity impacts can occur due to collision with another vehicle, vessel, or a submerged object. Ships operating in extremely cold climates require the removal of ice with large mallets or bats which can also generate low velocity impact damage.

Sandwich composites have been studied greatly under different shock loading conditions, including air blast [1–7]. It has been shown that the response of sandwich composites under these conditions is superior to the response of monolithic structures with the same areal density [7].

The effect of fire damage on the impact response of composites has been studied [8]. Ulven and Vaidya performed an experimental study coupled with a mechanical property estimation model to determine the effects of fire damage on the impact response of composite structures. Specimens included E-glass vinyl ester laminates and sandwich structures with E-glass vinyl ester face sheets and balsa wood cores. Both types of structures were exposed to an 800 °C flame for varying durations of time before being subjected to low velocity impacts. Impacts were imparted with a drop tower and with impact energy of 6.5 J. Composite specimens with 100s of exposure to the 800 °C flame, the peak force and contact stiffness in the laminates was reduced by 20–30%, and for the sandwich specimens a 65–75% reduction was observed.

* Corresponding author.
E-mail address: shuklaa@egr.uri.edu (A. Shukla).

1359-8368/$ - see front matter © 2010 Elsevier Ltd. All rights reserved.
doi:10.1016/j.compositesb.2010.09.005

Table 1
Properties of Corecell A800 [13].

Density range kg/m^3	Compressive strength (MPa)	Compressive modulus (MPa)	Shear strength (MPa)	Shear modulus (MPa)	Shear elongation (MPa)	Tensile strength (MPa)	Tensile modulus (MPa)
140–160	2.1	117	1.6	47	50%	2.5	183

Numerous studies have been performed on sandwich composites to determine the residual strength of the sandwich after impact but these were limited to a quasi-static compression after impact (CAI) experiments [9,10]. Schubel et al. have experimentally studied the effect of drop weight impacts on sandwich composites constructed of carbon fiber epoxy face sheets and PVC (Divinycell H250) cores. Impact energy was varied from 7.8 J to 108 J. After impact specimens were then subjected to a compression after impact. Delamination not visually detectable led to a decrease in compressive strength. Higher energy impacts were needed to develop significant damage with residual compressive strength less than 50% of the undamaged strength.

Similar compression after impact studies have been performed [11] as a means to create a damage assessment program specifically targeted at existing structures. Zenkert et al. focused on sandwich structures that are representative of structures in the Visby corvette, a fully composite naval vessel. Sandwich composites studied were composed of carbon vinyl ester face sheets and a PVC (Divinycell H80) core. Thin face sheets and thick face sheets were utilized. Two different impactors were used, one spherical and the other pyramid-shaped. Impact energy levels were 30–50 J for the specimens with thin face sheets and 100–250 J for the specimens with thick face sheets. CAI tests were performed on the impacted sandwiches. Damage levels reached in this study did not necessarily merit the repair of ship structures, as the aim was not to study the effect of impact on subsequent blast loads but the effect on normal operating loads in the structure for which the ship may be over-designed.

The effect of ballistic impact and the effect of explosive blast on the flexural properties of stitched composites have been studied by Mouritz [12]. The combined effect of both damage mechanisms was not studied. Stitching increased the mode I interlaminar fracture toughness but had little effect on the flexural properties or on reducing delamination due to high velocity impacts. Flexural properties of stitched laminates subjected to submerged explosive blasts showed improvements over unstitched laminates subjected to the same explosive levels.

Little experimental work has been done to characterize how sandwich composite structures with existing impact damage will perform during shock loading events. The experimental work presented here is used to compare low and high velocity impact damage determine what effects they have on sandwich structures during subsequent blast loading and identify what processes lead to structural failure under these conditions.

2. Experimental methods

Two different impact damage mechanisms were employed and their individual effects on subsequent air blast loading were studied. Sandwich composite specimens were first subjected to impact by either high velocity low mass projectiles or low velocity high mass drop weights. After impact experiments had been performed and acquired damage had been cataloged, the same specimens were subjected to blast experiments. The incident energy in these blast experiments was equal for all specimens. An undamaged specimen was also subjected to blast loading to use as a reference. Blast loading was performed with the use of a shock tube.

2.1. Materials

Sandwich composite specimens provided by The Material Science Corporation for this study were created using the SCRIMP process and consisted of laminate face sheets and a Styrene Acrylo-Nitrile (SAN) foam core. The face sheets were constructed with a vinyl ester matrix and 24 *oz*/*yd*^{2} E-Glass woven roving in a layup of $[0/45/90/-45]_s$. The core was Corecell A800 manufactured by Gurit. Corecell A series foams used as a core exhibit good performance under dynamic loads due to excellent shear properties. The properties of Corecell A800 as provided by the manufacturer are listed Table 1 and experimental results for the static and dynamic constitutive behavior as obtained in laboratory experiments are shown in Fig. 1. The dynamic properties were obtained using the Split Hopkinson Pressure Bar apparatus.

Overall specimen's dimensions were $102 \times 254 \times 60$ (mm) with a face sheet thickness of 5 mm. The average areal density of the specimens was 27.9 kg/m^2. An image of a specimen is shown in Fig. 2.

2.2. High velocity impacts

High velocity impacts were obtained by way of a 300 Winchester Magnum rifle firing into an enclosed test chamber where the specimen was held under clamped conditions on the top and bottom edges. The bullets used in this study were 165 grain, stainless steel, copper jacketed, armor piercing bullets (APM2). This type of bullet was chosen over a softer bullet to ensure that the bullet would pass though the specimens undamaged and absorb no energy in the process. By choosing a bullet that is not damaged during impact, the change in kinetic energy of the bullet can be equated to the energy absorbed by the specimen during the impact event. The elastic response of the specimen can be ignored based on Skvortsov's findings [14]. An assumption is made that initial rotation of the bullet about its long axis due to rifling in the gun barrel and any change to that rotation during impact is small enough to be ignored. The same holds true for any rotation imparted to the bullet during impact and present after the bullet has exited the specimen.

The velocity of the bullets was measured with velocity traps positioned in front of the specimen and behind the specimen as shown in Fig. 3. A timing box and a digital oscilloscope were used to record the events. Given the impact velocity and exit velocity of the bullet the change in kinetic energy of the bullet can be known and therefore the energy absorbed by the specimen is known.

Five specimens were subjected to varying high velocity impacts ranging from one to five as shown in Fig. 4. Thus, each specimen had a different level of impact damage. All impact locations were offset 25.4 mm from the center lines of the specimens except for specimens impacted with one bullet and five bullets as they required an impact in the center of the specimen for symmetry.

To confirm that the bullets were exiting the specimen undamaged, high speed photography was employed. With the use of a mirror, images were taken simultaneously of the impact face and exit face. Fig. 5 shows an overhead view of a specimen, velocity trap break screens, projectile path, mirror, and camera angle. The right image offers an explanation of captured images. Fig. 6 shows

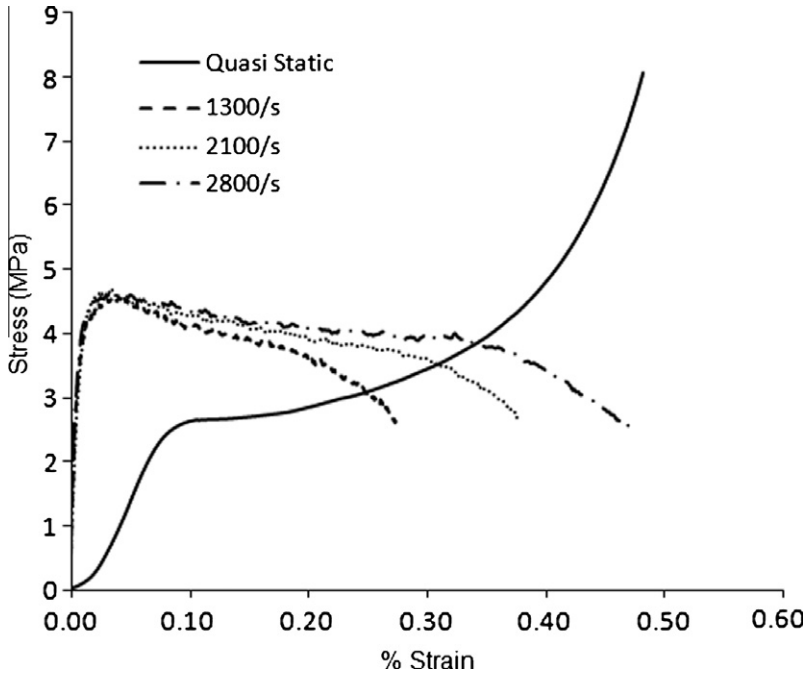

Fig. 1. Quasi-static and dynamic constitutive properties of Corecell A800.

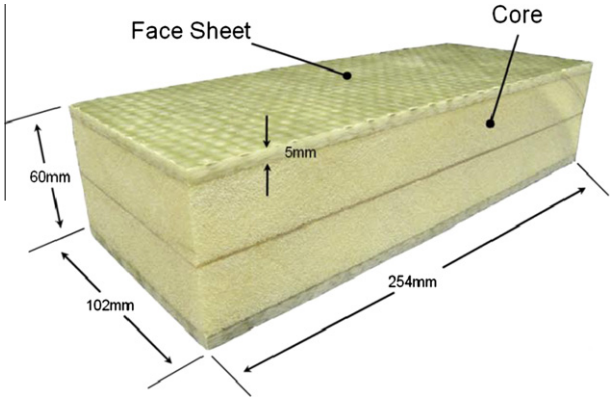

Fig. 2. Image of sandwich composite specimen and dimensions.

high speed images of a bullet before and after impact. The bullet is undamaged after impact confirming that the change in kinetic energy can be equated to the energy absorbed by the specimen.

2.3. Low velocity impacts

Low velocity impact damage was created with an Instron Dynatup 9210 drop tower. The Dynatup 9210 used is outfitted with a medium weight crosshead and is capable of producing 4.6–300 J of energy. The maximum impact velocity that can be achieved is 5 m/s. The drop tower is equipped with a data acquisition system including a velocity detector, a piezoelectric tup for measuring loads, a signal conditioning amplifier, and a computer. Due to impact event duration, a 20 ms sampling time was chosen which corresponds to a sampling rate of 410 kHz. The system is capable of measuring impact velocity as well as rebound velocity.

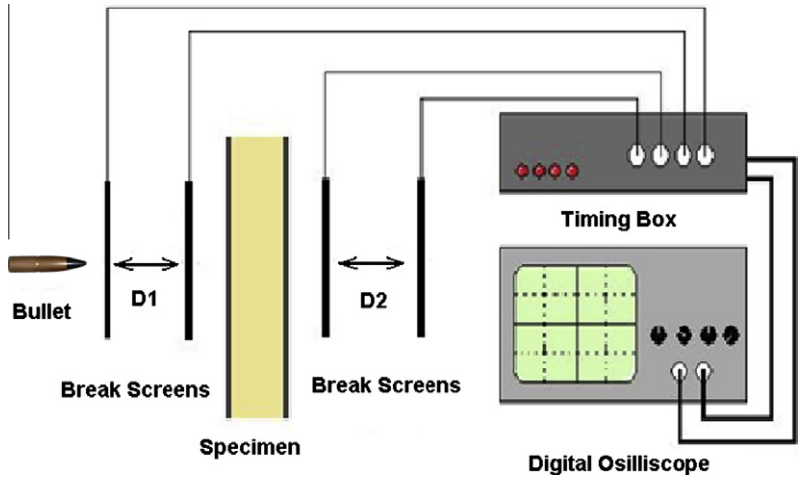

Fig. 3. Schematic of the experimental set up for high velocity impacts.

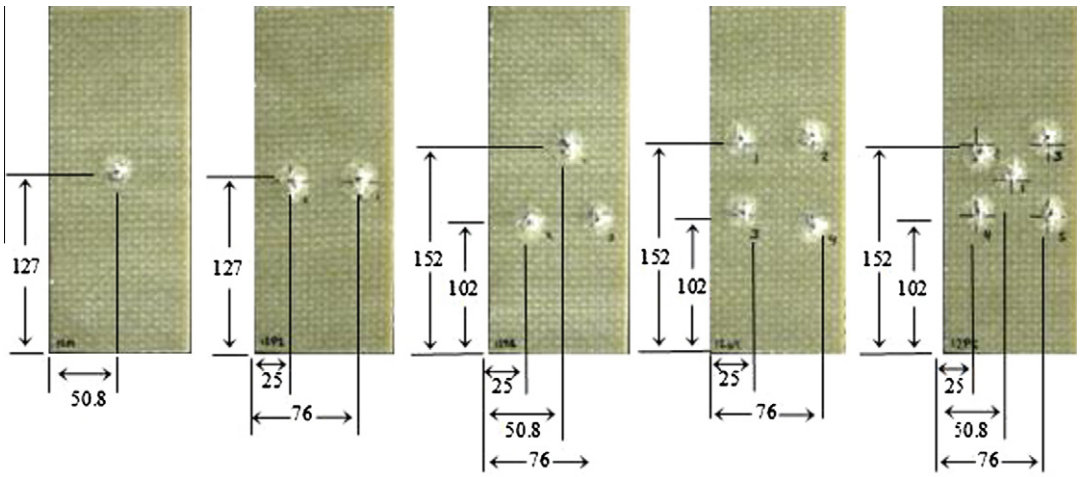

Fig. 4. Impact locations for high velocity impacts (dimensions in mm).

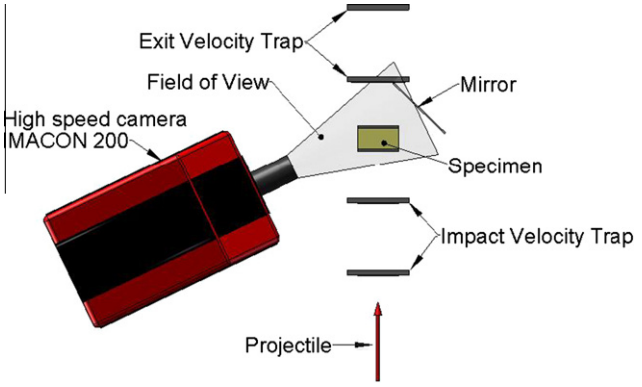

Fig. 5. Top view of high velocity impact experiment set up with Imacon 200 high speed camera.

Sandwich specimens were subjected to 300 J low velocity impacts with a 25.4 mm (1in) diameter hemispherical striker installed on the tup. The mass of the drop weight was 26.16 kg and was dropped from a height of 1.16 m. Fig. 7 shows the drop tower and a specimen placed in the simple supports with the hemispherical impactor in contact with the specimen.

Three specimens were subjected to low velocity impacts. The number of impacts per specimen was varied from 1 to 3. The locations of the impacts for each specimen are shown below in Fig. 8. Impacts were located within a 76 mm diameter circle centered on the specimen. This area corresponds to the loading area of the shock tube which would be used in the subsequent blast loading experiments.

After the initial impact on the specimen the cross head and striker can rebound and impact the specimen an additional number of times. To avoid secondary impacts, a string was tied to the specimens and when the striker and cross head rebounded the specimen was quickly pulled from the fixture manually before the specimen could be loaded again.

2.4. Shock tube

For all blast loading experiments a shock tube was utilized to simulate shock loading from an explosive event. The shock tube is a long tube open at one end and closed at the other and is divided into two main sections, the driver section and the driven section as shown in Fig. 9. The two sections are separated by a diaphragm. To operate the shock tube, the driver section is pressurized with an inert gas until the diaphragm separating the driver

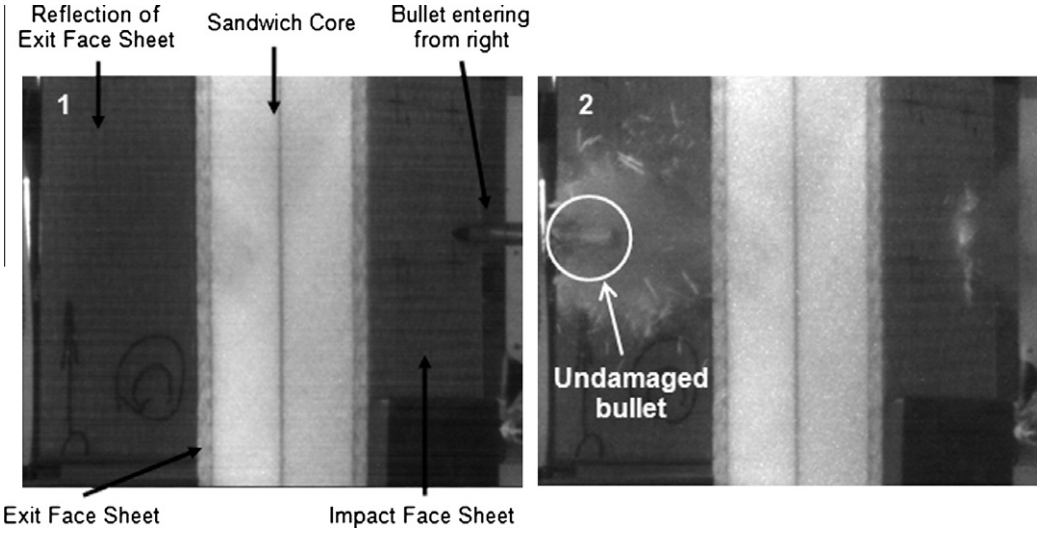

Fig. 6. High speed images of bullet impact showing the entry (image 1) and the undamaged bullet exiting the specimen (image 2).

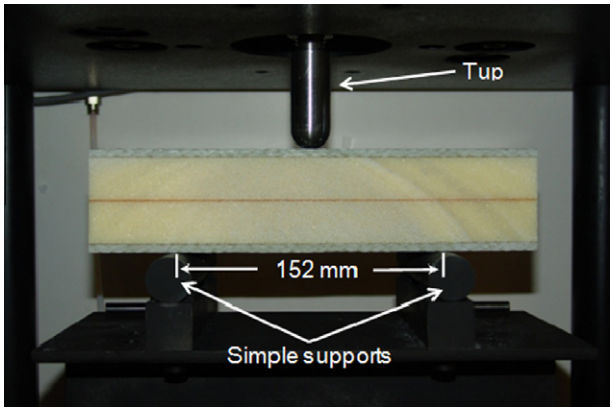

Fig. 7. Specimen placed in simply supported condition for low velocity impact.

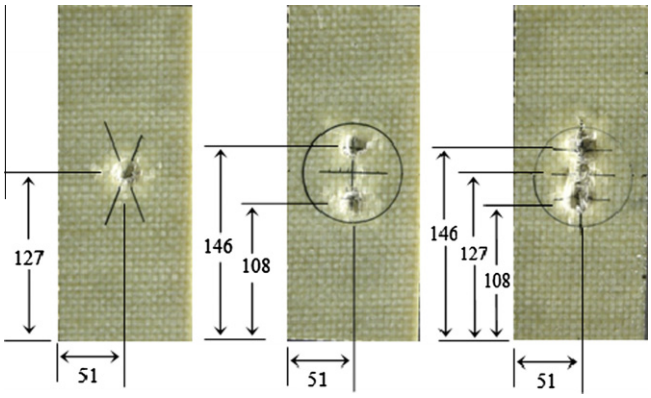

Fig. 8. Impact locations for low velocity impacts.

section and driven section ruptures. Upon rupturing, the expansion of gas into the driven section creates a shock wave that travels down the tube toward the open muzzle where the specimen is located. The specimens were held in simply supported conditions as shown in Fig. 10. The span of the supports was 152 mm and the ID of the shock tube is 76 mm. The muzzle of the shock tube is instrumented with two pressure transducers located at different distances from the end of the tube. By using two transducers, both pressure at the specimen and shockwave velocity can be measured. Fig. 10 shows a schematic of the end of the shock tube, a specimen and the two pressure transducers. The pressure transducers are output to a signal conditioner and from there to a digital oscilloscope. With the use of the oscilloscope the entire pressure time history of the blast event was recorded. All blast loading was performed at the same level. The blast generated pressure wave had a peak amplitude of 2 MPa and a velocity of 1340 m/s. This generated a reflected shock pressure with a peak of about 8.5 MPa. This reflected pressure is a measure of the loading applied to the specimen [15].

3. Results and discussion

3.1. High velocity impact

Images of typical damage to impact face sheets and exit face sheets are shown in Fig. 11. Damage to the impact face sheet is confined to an area approximately 25 mm in diameter and include, puncture, delamination, fiber breakage and matrix cracking. Damage to the exit face sheet is more extensive covering 50 mm diameter area with more extensive fiber breakage, matrix cracking and delamination.

In order to study the distribution of damage through the thickness of the sandwich, a postmortem dissection was performed. A specimen was sectioned after impact by high velocity projectiles. Both the impact and exit face sheets were cut from the core with a band saw. Fig. 12 shows how the specimen was sectioned, the nomenclature for surfaces and damage to the interior of the sandwich specimen after high velocity impact. Damage to the core on both impact and exit sides is similar and is composed of puncture the same diameter of the projectile. This is to be expected as the shear strength of the core is small and the bullet can easily penetrate through it by sheering the walls of the hole. The interior of the impact face sheet and exit face sheet include puncture and a

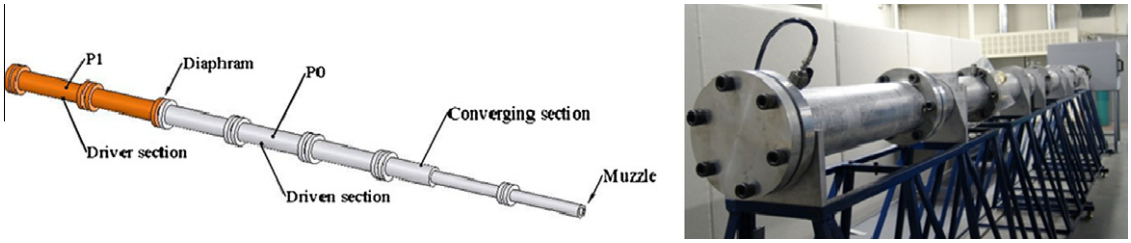

Fig. 9. Diagram and image of shock tube.

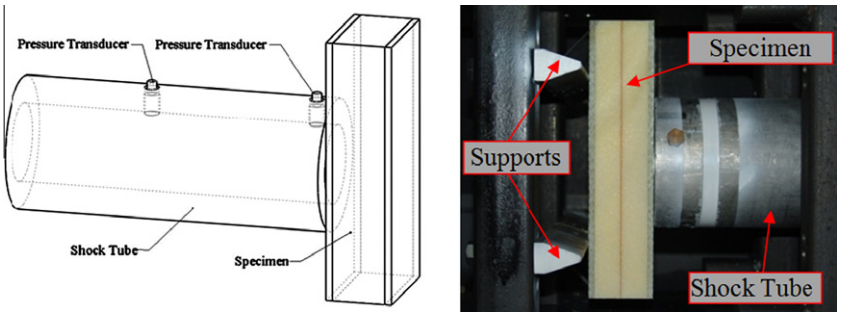

Fig. 10. (Left) Schematic of muzzle section showing transducers. (Right) Image of specimen and shock tube.

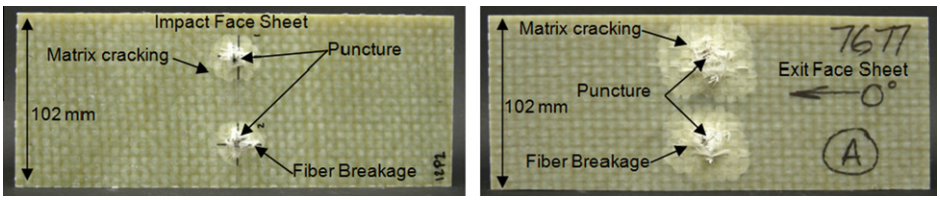

Fig. 11. (Left) Typical impact face sheet damage from high velocity impact (Right) Typical exit face sheet damage.

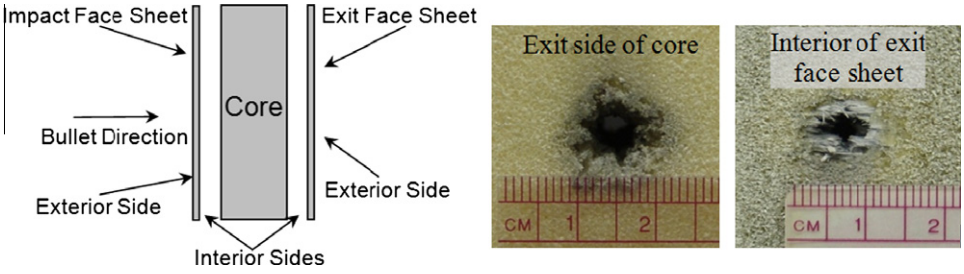

Fig. 12. (Left) Sectioning of specimen for post mortem damage study (Right) High velocity damage on interior of specimen.

small area of delamination approximately twice the diameter of the projectile. Damage to the exit face sheet increases through the thickness of the sheet with less damage to the interior and greater damage to the exterior. This phenomenon is discussed in Mouritz [12]. As the bullet passes through the exit face sheet the laminate is able to develop greater out of plane strain near the exterior surface of the exit face sheet as it is an unsupported free surface. Interlaminar failure develops as a result of the out of plane strain and in plane tensile loads develop as well and create the fiber breakage and matrix cracking.

For each high velocity impact the change in kinetic energy of the projectile is equated to the energy expended in the process of damaging the specimens. Taking averages of the change in kinetic energy for each impact number reveals a decreasing trend in energy absorption for each subsequent high velocity impact a specimen experiences. Delamination of the exit face sheet due a high velocity impact reduces the mode I interlaminar fracture toughness by introducing interlaminar cracks. Once the fracture toughness has been reduced less energy is required to produce similar amounts of damage as the previous impact, producing the trend seen in Fig. 13. On average, a specimen absorbs 650 J of energy from the first impact, decreasing linearly to 200 J for the fifth impact.

3.2. Low velocity impact

Damage due to low velocity impact included puncture at the impact site, delamination to the immediate area around the puncture and matrix cracking. Puncture of the impact face sheet was generated by out of plane compressive loads and in plane tensile loads while delamination can be attributed to interlaminar shear failure due to localized bending at the impact site. The low velocity impacts also generated de-bonding of the core and impact face sheet as seen in Fig. 14, along with typical impact face sheet damage. Face sheet core de-bonding may be due to tensile stresses created by stress waves propagating from the high impedance face sheet to the low impedance core material.

After impact, core damage was investigated by sectioning a specimen with damage from one low velocity impact. Fig. 15 shows the impact side of the core after impact and sectioning with a band saw. The core exhibits only localized crushing due to face sheet failure. Fiber in the indentation is still partially bonded to the core.

A typical load time history of a low velocity impact event and the energy associated with it are shown in Fig. 16. Event duration is approximately 12 ms with a maximum load of 31 kN. The peak load drops at 2.75 ms corresponding to face sheet failure. Load

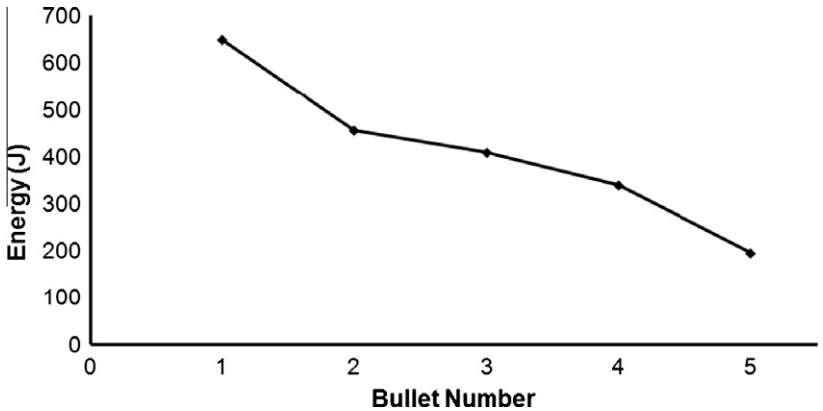

Fig. 13. Average change in kinetic energy for each high velocity impact.

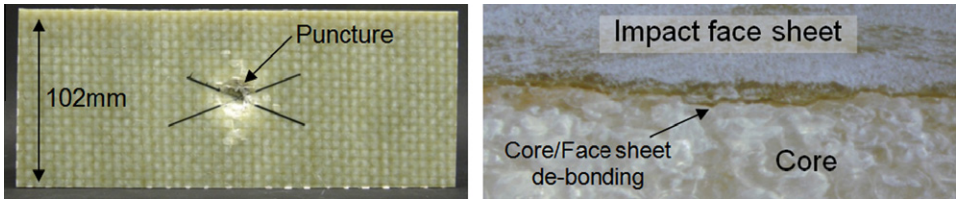

Fig. 14. Typical low velocity impact damage. (Left) Face sheet. (Right) Core/face sheet de-bonding.

Fig. 15. Core damage due to low velocity impact.

then increases again slightly due to local densification of the foam core and subsequently drops monotonically to zero.

For each low velocity impact total energy absorbed in the impact process was extracted from the collected data and the results are shown in Table 2. Load data acquired from the piezoelectric tup can be used to find the energy absorbed by the specimen by numerically integrating the load with respect to time as in Eq. (1), where V_1 is the impact velocity, F is the load and m is the drop weight mass.

$$E(t) = \frac{m}{2}\left(2V_1 \int \frac{F}{m}dt - \left(\int \frac{F}{m}dt\right)^2\right) \quad (1)$$

No decreasing trend in energy absorbed for additional impacts is seen during low velocity impact experiments. On average low velocity impacts created 252 J of impact damage per impact. The total energy absorbed by the specimen subjected to three low velocity impacts was 761 J.

3.3. Blast loading

Three different groups of specimen were subjected to blast loading. The first was an undamaged specimen. The second group included five specimens that had been subjected to high velocity impact prior to blast loading. The third group was composed of three specimens that had been subjected to low velocity impacts prior to blast loading. Pressure data and high speed images were captured during blast loading. Fig. 17 shows six images of the blast loading event of an undamaged specimen taken at a framing rate of 11,000 fps. Shear cracking has developed in the core by 360 μs. Blast loading of an undamaged sandwich specimen produced 14 mm of deflection and a reflected peak pressure of about 8.5 MPa. Post blast images of an undamaged sandwich composite are shown in Fig. 18. The impact face sheet and exit face sheet ex-

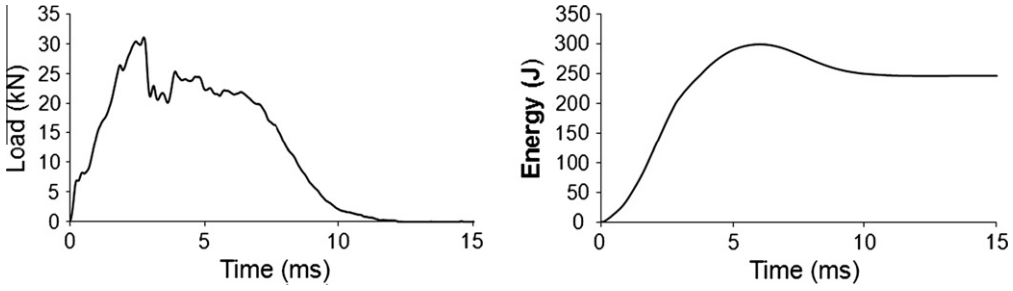

Fig. 16. Typical low velocity impact load and corresponding energy.

Table 2
Low velocity impact experimental data.

Specimen	Impact	Maximum load (kN)	Impact velocity (m/s)	Rebound velocity (m/s)	Energy absorbed (J)	Energy absorbed/ specimen (J)
1 Impact	1	31.0	4.76	1.73	255	255
2 Impact	1	29.9	4.77	1.90	247	496
	2	34.4	4.76	1.85	249	
3 Impact	1	30.7	4.78	2.61	208	761
	2	23.1	4.78	1.20	278	
	3	29.4	4.78	1.25	276	

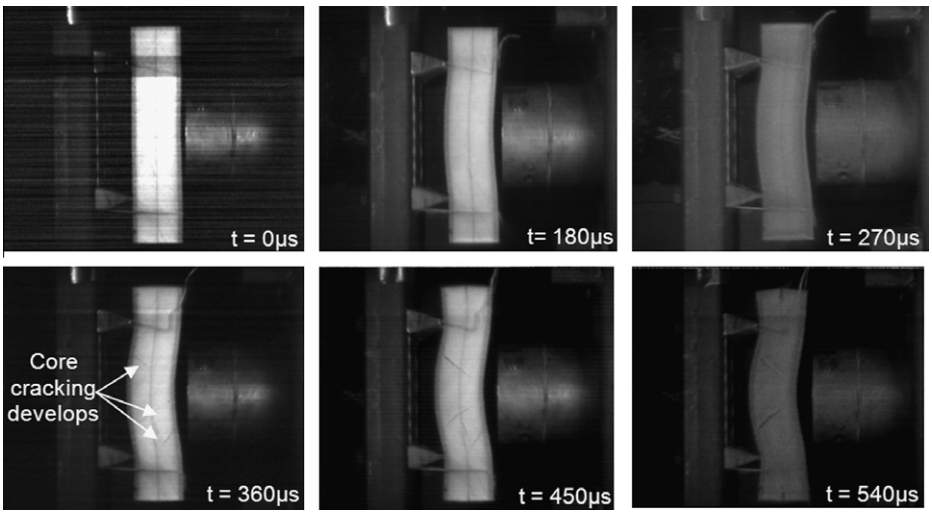

Fig. 17. Blast loading of an undamaged specimen.

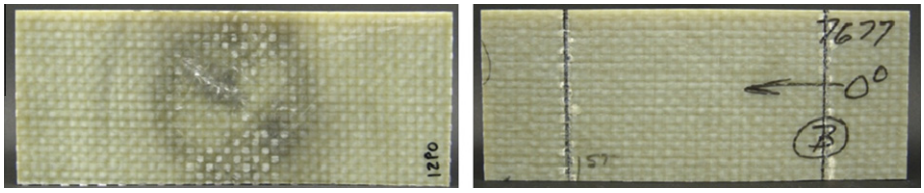

Fig. 18. Post blast image of impact face sheet and back face sheet.

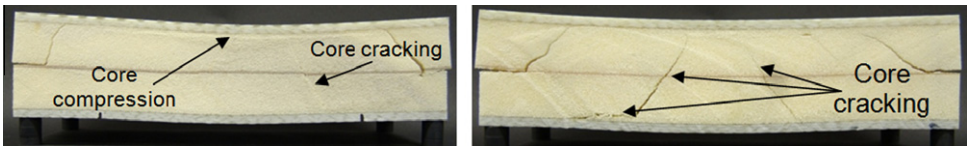

Fig. 19. Post blast images of core.

hibit no damage while the core, shown in Fig. 19, has shear cracks and core compression adjacent to the impact face sheet.

Specimens that had previously been damaged by high velocity impacts were subjected to an incident blast wave with a peak pressure of 2 MPa and a velocity of 1340 m/s. High speed images of a specimen that had been damaged by five high velocity impacts are in Fig. 20. Large core compression begins by 90 μs while shear cracking does not develop until 720 μs. During blast loading the reflected pressure was approximately 8.5 MPa and the specimen reached a maximum deflection of 16 mm. Fig. 21 shows post blast

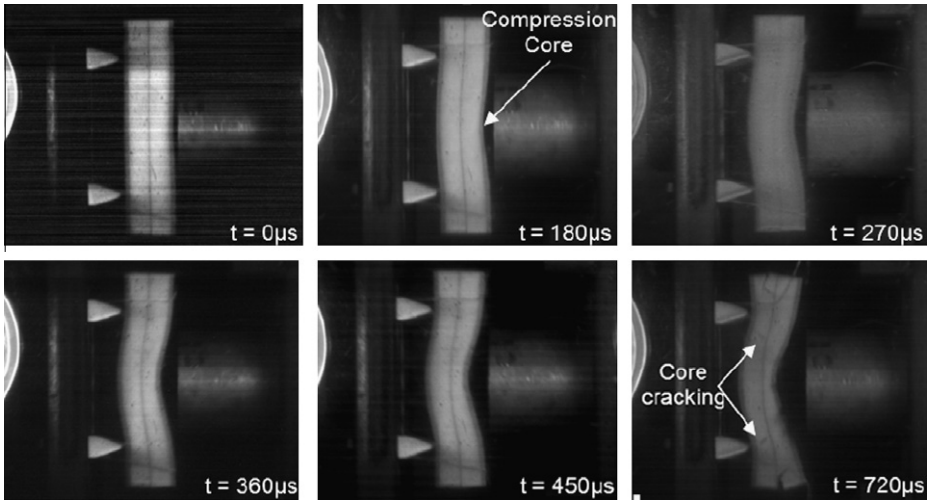

Fig. 20. Blast loading of a specimen with a high level of high velocity impact damage. Energy absorbed during impact experiments = 2108 J.

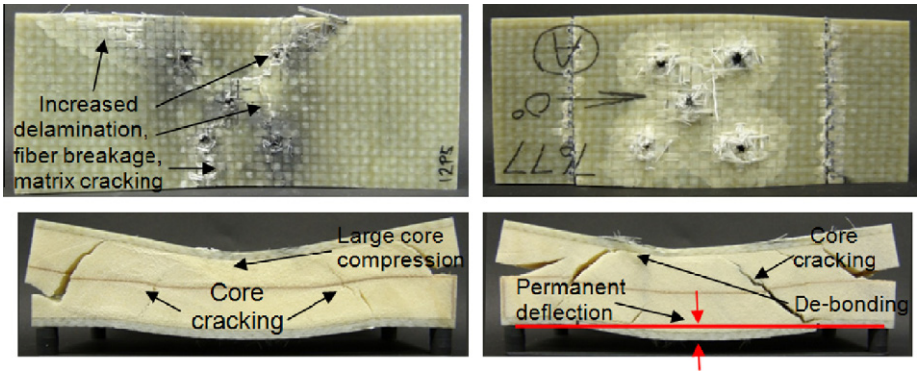

Fig. 21. Post blast image of a specimen with a high level of high velocity impact damage.

images of the specimen with damage from five high velocity impacts and blast loading. On the impact face sheet delamination from the impact sights has propagated toward the edge of the specimen and fiber breakage and matrix cracking have increased. The image on the top right, in Fig. 21, shows no increase in the damage created by high velocity impacts on the exit face sheet due to blast loading. The dominant effect of the blast loading is to the core which has developed shear cracks and core compression adjacent to the impact face sheet. A higher degree of permanent deflection in comparison to the specimen with no impact damage is evident.

Sandwich composite specimens that had previously been subjected to low velocity impacts were subjected to a secondary blast loading experiment. The blast loading was equal in magnitude to the blast experiments performed on a specimen with no damage and specimens that had damage from high velocity impacts. In this experiment a newly purchased Photron SA-1camera was used to photograph the blast event. Fig. 22 shows high speed images

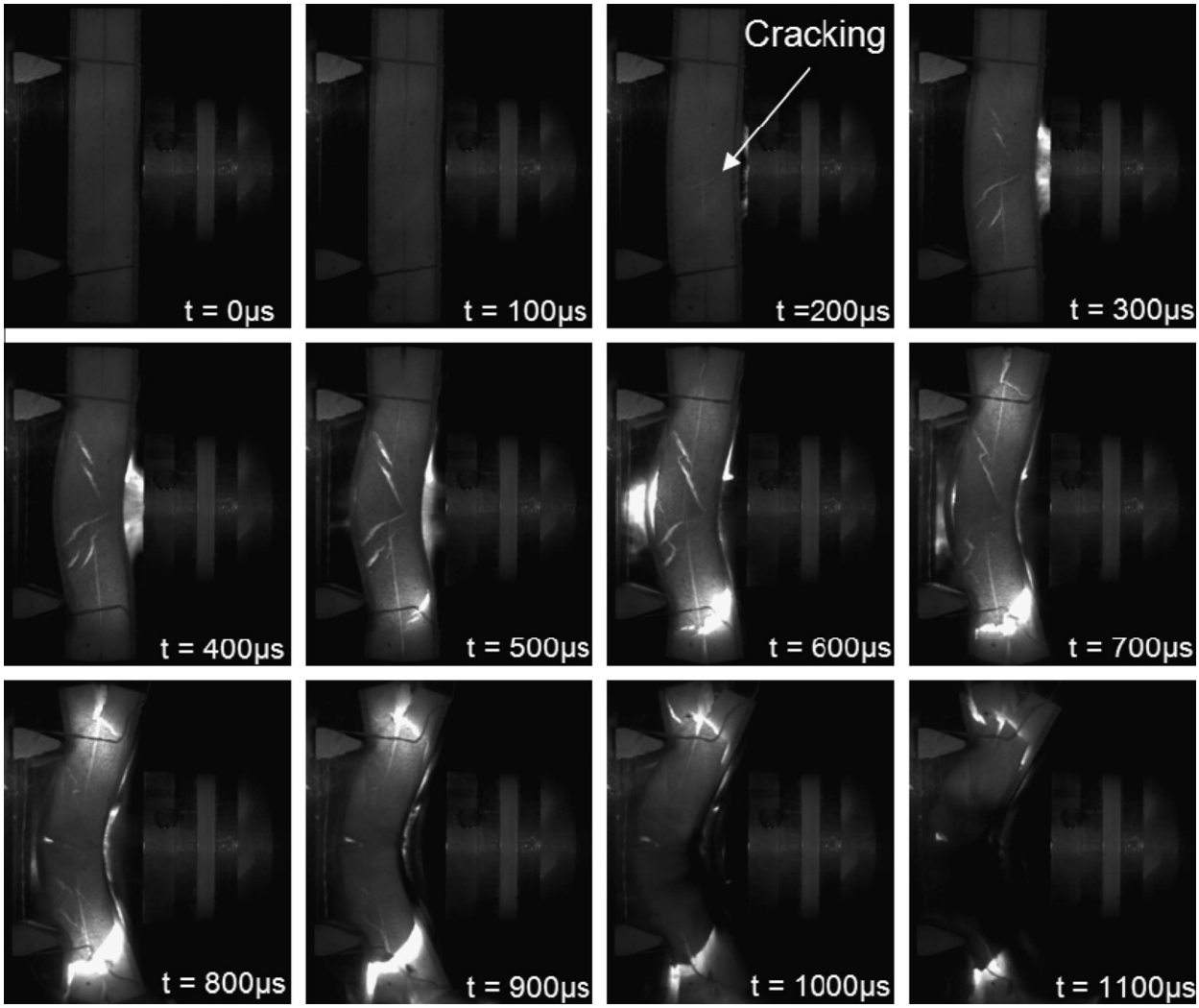

Fig. 22. Blast loading of a specimen with damage from three low velocity impacts.

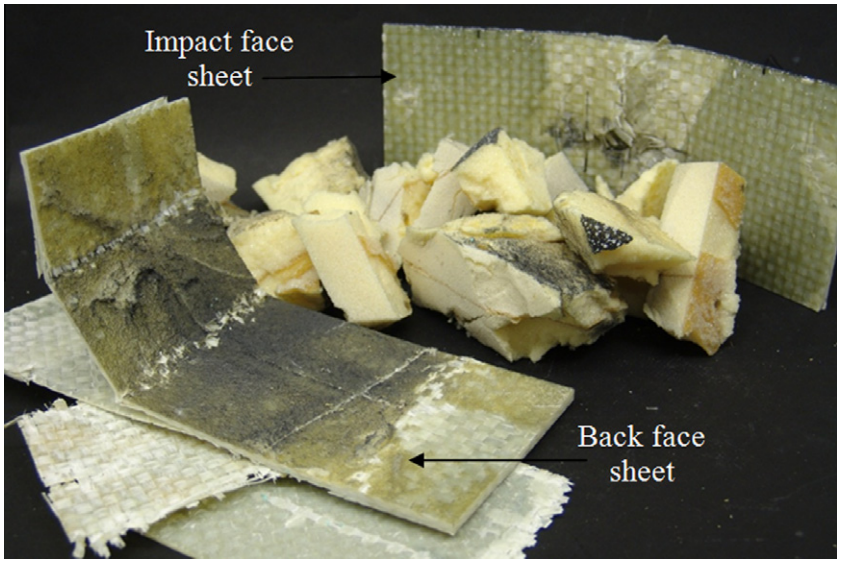

Fig. 23. Post blast image of a specimen that had been subjected to three low velocity impacts and a subsequent blast loading.

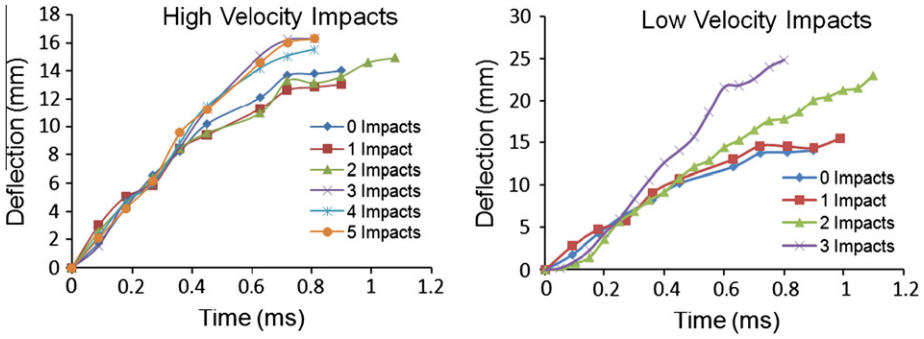

Fig. 24. Deflection of back face sheet during blast loading of specimens with high velocity impact damage (left) and low velocity impact damage (right).

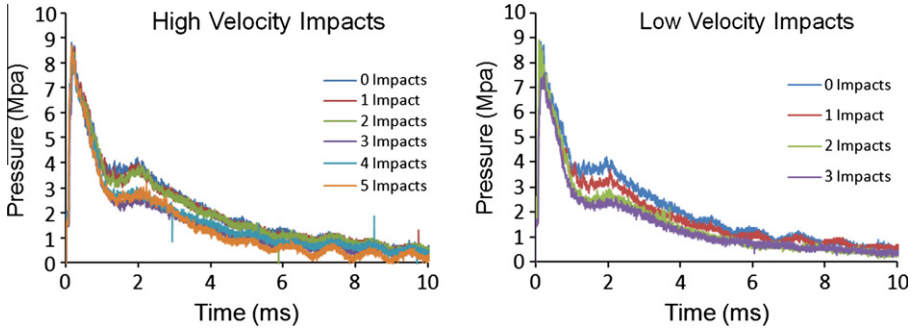

Fig. 25. Pressure time history of blast loading specimens with high velocity impact damage (left), and low velocity impact damage (right).

captured during blast loading of a specimen with damage from three low velocity impacts equal to a total absorbed energy of 761 J; much less than the specimen with damage from five high velocity impacts (2108 J) discussed above. Blast loading of the specimen produced a reflected pressure of approximately 7.5 MPa. The specimen experienced complete failure with core cracking evident by 200 μs and de-bonding of the back face sheet by 500 μs. The de-bonding between the impact face sheet and core that was present due to low velocity impacts reduced specimen stiffness which significantly impaired the sandwiches ability to support compressive loads during bending. Large puncture to the impact face sheet allowed high pressure gas to infiltrate the core and then propagate throughout the core causing core failure, de-bonding of the exit face sheet and ultimately, complete specimen failure.

A post blast image of the specimen that had been subject to three low velocity impacts and a 2 MPa blast loading is shown in Fig. 23. The specimen experienced de-bonding of the face sheets from the core and complete failure during blast loading. Separation of the back face sheet lamina seen in Fig. 23 can be attributed to interlaminar shear failure due to large bending at the simple supports as seen in the high speed images. Large compressive loads due to bending cause failure of the impact face sheet.

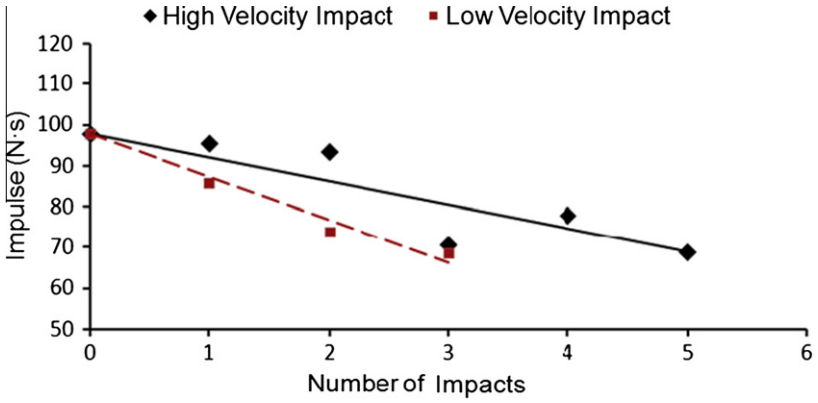

Fig. 26. Impulse generated from blast loading pressure data.

High speed images captured during blast loading were used to generate real time deflection data for each specimen. Deflection was measured at the point of maximum deflection on the back face sheet of each specimen. Fig. 24 shows the deflection of specimens during blast loading with damage from high velocity impacts as well as deflection data for specimens with damage from low velocity impacts. When back face sheet deflection is used as a measure of specimen performance during blast loading, specimens with damage from low velocity impacts performed worse than those with damage from high velocity impacts even though specimens with low velocity impact damage were subject to fewer impacts and absorbed less energy during impact events. Each low velocity impact generated, on average, 252 J of energy in the specimen while the first high velocity impact generated 650 J of energy in the specimen. The specimen with the most low velocity impact damage had accumulated 761 J of damage before blast loading while the specimen with the most damage from high velocity impacts had accumulated 2108 J of damage.

Pressure data collected during blast loading from the sensor next to the specimen is shown in Fig. 25. This pressure data was utilized as a measure of specimen performance. Given the same incident shock wave, a more compliant specimen will reflect less energy back down the shock tube generating a lower reflected pressure and impulse. By numerically integrating the pressure data, the impulse experienced by the specimens is obtained using the Eq. (2),

$$I = A \int Pdt \tag{2}$$

where I is the impulse, A is inner diameter of the shock tube and P is the reflected pressure.

Fig. 26, shows the impulse from blast loading both types of specimens, those with high velocity impact damage and those with low velocity impact damage. The impulse shown for the specimen with no impact damage is common to both high and low velocity series. Both plots show a decreasing trend while the impulse for the specimens with low velocity impact damage has a greater slope. In regards to blast performance, the impulse data agrees well with the deflection data that was extracted from the high speed images.

4. Conclusions

The blast performance of sandwich composite specimens with damage from either high velocity low mass impacts or damage from low velocity high mass impacts were compared to the blast performance of a sandwich specimen with no impact damage. Data collected during the experiments shows the following;

(1) Damage incurred during high velocity impacts was most prominent on the exit face sheet of the sandwich composite specimens while specimens subjected to low velocity impacts developed damage that was confined to the impact face sheets and cores.
(2) Specimens that were struck by high velocity projectiles absorbed a higher level of energy during the impact process as compared to the specimens struck by low velocity high mass drop weights.
(3) Experiments show that the damage to the front face sheet is more detrimental to the performance of the sandwich composite than the damage to the back face sheet.
(4) The performance of the sandwich specimen previously subjected to high velocity impacts is superior to the blast performance of sandwich composite specimens previously subjected to low velocity high mass impacts.

Acknowledgements

The authors acknowledge the financial support provided by the Office of Naval Research (Dr. Yapa D.S. Rajapakse) under Grant # N000140410268 and the Department of Homeland Security under the Cooperative Agreement # 2008-ST-061-ED000. Specimens used in this study were provided by The Material Science Corporation.

References

[1] Tekalur SA, Bogdanovich AE, Shukla A. Shock loading response of sandwich panels with 3-D woven E-glass composite skins and stitched foam core. Compos Sci Technol 2008;69(6):736–53.
[2] Andrews EW, Moussa NA. Failure mode maps for composite sandwich panels subjected to air blast loading. Int J Impact Eng 2009;36(3):418–25.
[3] Nurick GN, Langdon GS, Chi Y, Jacob N. Behavior of sandwich panels subjected to intense air blast – part 1: experiments. Compos Struct 2009;91(4):433–41.
[4] Wang E, Gardner N, Shukla A. The blast resistance of sandwich composites with stepwise graded cores. Int J Solids Struct 2009;46(18–19):3492–502.
[5] Tekalur SA, Shukla A, Shivakumar K. Blast resistance of polyurea based layered composite materials. Compos Struct 2008;84(3):271–81.
[6] Lan S, Lok T, Heng L. Composite structural panels subjected to explosive loading. Constr Build Mater 2005;19(5):387–95.
[7] Zhu F, Lu G. A review of blast and impact of metallic and sandwich structures. EJSE Special Issue: Loading on Structures; 2007. p. 92–101.
[8] Ulven CA, Vaidya UK. Impact response of fire damaged polymer-based composite materials. Composites: Part B 2008;39(1):92–107.
[9] Schubel PM, Luo JJ, Daniel M. Impact and post impact behavior of composite sandwich panels. Composites: Part A 2007;38(3):1051–7.
[10] Davies GAO, Hitchings D, Besant T, Clarke A, Morgan C. Compression after impact strength of composite sandwich panels. Compos Struct 2004;63(1):1–9.
[11] Zenkert D, Shipsha A, Bull P, Hayman B. Damage tolerance assessment of composite sandwich panels with localized damage. Compos Sci Technol 2005;65(15–16):2597–611.

[12] Mouritz AP. Ballistic impact and explosive blast resistance of stitched composites. Composites: Part B 2001;32(5):431–9.
[13] Corecell a foam structural core material product data sheet. PDS-Corecell A-Foam-5-0905. <www.Gurit.com>.
[14] Skvortsov V, Kepler J, Bozhevolnaya E. Energy partition for ballistic penetration of sandwich panels. Int J Impact Eng 2003;28(7):697–716.
[15] Jackson M. The performance of damaged sandwich composites under blast loading conditions, MS Thesis, University of Rhode Island; 2009.